Chapter 6

DEVELOPMENT AND ANALYSIS OF A HIGH-SPEED VALVE MODULATOR FOR FAST COMPREHENSIVE TWO-DIMENSIONAL GAS CHROMATOGRAPHY

Introduction

Pneumatic modulation of carrier gas velocities at the junction point between two separation columns to enhance chromatographic separations were pioneered in the Sacks lab at the University of Michigan.(D, E, F) This work involved using an electronic pressure controller to vary the pressure at the junction point which yielded additional flexibility in controlling the flows along the second column. This additional controllable parameter provided another way to shape elution profiles and tune the separation to resolve critical pairs. This work culminated in the development of the stop flow technique where pressure equal to the inlet pressure is applied to the junction point, effectively stopping the flow through the first column and accelerating the flow along the second column.(A,B,C) Compounds that are not nominally separated due to inverse migration behavior along the two columns can be separated with judicious application of pressure pulses, since one compound will experience heightened speed on the second column while the other will be stopped on the first column. All compounds on the first column are stopped and will not suffer any separation loss aside from some longitudinal band broadening; the only significant sacrifice is some additional run time. Gorecki was among the forerunners to use this stop-flow technique explicitly for GCxGC operation.(J) By operating the second column flow independently, the second column separation time can be fine-tuned. (*this sentence belong here or with the other valve modulator forerunners?)*

Valve modulators offer key advantages over thermal modulators for high-speed and/or portable applications. First, the switching times (often a few ms or less) of valves

are typically significantly faster than thermal modulators. This is because the mechanical mechanisms can be actuated more quickly than the large temperature changes required for thermal modulation to be achieved. Once actuated, the flow equilibrates rapidly allowing high-speed modulation of the flow. Second, the resources required to operate valve modulators are typically only electrical energy. This is a significant advantage over cryogen-dependent thermal modulators for applications requiring a portable system. The third advantage to valve modulators is the independence of modulation efficiency from partition coefficients or trapping characteristics. Equation 6.1 shows the migration band

$$u_{z,i} = \frac{u_z}{(1+k_i)} \tag{6.1}$$

velocity, $u_{z,i}$, at a modulator at position z along the column ensemble where u_z is the linear velocity at position z along the column and k_i is the retention factor of the ith compound. Because the modulation is performed by altering the flow rate rather than thermal trapping, a compound's affinity for the modulator's surface is irrelevant in terms of how well the compound behaves in the modulator. This allows for straightforward modulation of light compounds such as methane and sulfur dioxide which are notoriously difficult to thermally trap. Furthermore, breakthrough of components from poor trapping is a non-issue.

Bruckner and co-workers used the first 6-port valves for GCxGC.(G) Sample eluting from the first column would pass through a sample loop and then vent to the atmosphere, and when the valve actuated, a secondary pressure source flushed out the sample loop into the second column. This system did have a weakness in that sample loss through the vent was significant. Seeley and co-workers developed this idea further, known as differential flow modulation, by operating the first column at a low flow rate

and the second column at a much higher rate to both reduce sample lost to vent and to focus the injection plug width for second column separation.(H) Seeley then refined the design using two sample loops to prevent any sample loss and also located the valve outside the sample pathway, preventing valve material from influencing the separation. (I)

This chapter will describe the functionality and performance of a Sandia-proprietary rotor-based valve developed for both high-speed analysis and portability. Experiments demonstrating methane modulation and peak area conservation are described, and analyses regarding peak width and peak capacity are provided. Finally, an 18-component mixture consisting of compounds with a variety of functional groups is separated in under 9 s using this valve.

Experimental Section

Apparatus. Figure 6.1 displays the system diagram. All studies were carried out using an Agilent (Wilmington, DE) 6890 gas chromatograph equipped with a 7683B Series auto-injector and a flame-ionization detector (FID). All experiments were performed with the oven temperature at 25º C. In order to achieve a data acquisition rate of 1000 Hz, the stock electrometer circuitry was replaced with a 22.5 V Eveready (St. Louis, MO) No. 412 NEDA 215 battery for bias voltage to the FID and a Femto Messtechnik GmbH (Berlin, Germany) DLPCA-200 electrometer for current-to-voltage signal conversion and amplification.

The heated transfer lines were created by running nichrome heating wire (Omega Engineering, INC., Stamford, CN) through fiberglass sleeving (FBGS-R-30 from Omega) to prevent electrical shorts. This insulated heating wire was threaded through another layer of fiberglass sleeving (XC·18 from Omega) along with the deactivated 0.100 mm

i.d. capillary (Restek, Bellefonte, PA) transfer lines. Nanovolume unions from VICI Valco Instruments, Co. (C-NEU.5XFPK, Houston, TX) were used to connect the transfer line capillary tubing to the 0.150 mm i.d. capillary leads epoxied into the microfabricated column. Once all the connections were finalized, a final layer of fiberglass insulation tape (PN# 01-472A, Fisher-Scientific), was wrapped around the transfer line and valve connections. The transfer line was heated using a Hewlett Packard (Palo Alto, CA) E3610A DC Power Supply set to 13.5 V to achieve ~110º C. Temperature was monitored using a K-type thermocouple from Omega.

Data was recorded on a Dell Precision M6300 laptop computer with an in-house data acquisition program created in LabVIEW 8. A National Instruments (Austin, TX) NI USB-6009 data acquisition board was used to facilitate data acquisition and control relays. Additional electronic connections were made using a 3M (St. Paul, MN) solderless breadboard powered with 5 V using a Hewlett Packard 6216B power supply. Data collected was processed using GRAMS/AI 7.00 (ThermoGalactic, Waltham, MA) for one-dimensional processing and Origin Pro 7.5 (Originlab Corporation, Northampton, MA) for two-dimensional processing.

The microfabricated columns are created through deep reactive-ion etching (DRIE) into a silicon wafer to create the grooves that become channels after a glass lid is anodically bonded to the top of the wafer. These channels are 30 um wide x 685 um tall, and have total channel lengths of 90 cm for the 3090-type columns and 30 cm for the 3030-type columns. To prepare the microcolumns for use, capillary leads of 0.150 mm i.d. and 0.660 mm o.d. from Polymicro Technologies, L.L.C. (Phoenix, AZ) (Part# 2001815) were epoxied into place using Loctite 1C Hysol Epoxi-patch Adhesive (Henkel, Düsseldorf, Germany) and letting it sit in a 60º C oven for 2 hours for curing.

Afterwards, Minco heaters (HK5572R13.9L12E(-) for 3090 and HK5565R10.0L12E(-) for 3030 columns) (Minneapolis, MN) were placed on the top and bottom faces of the microcolumns. Each pair of heaters on a column were powered by an Agilent E3648A Dual Output DC Power Supply. K-type thermocouples from Omega were used to measure column temperature, and Fluke (Everett, WA) 80TK Thermocouple Modules were used to interface the thermocouples with the DAQ hardware.

The valve modulator is a proprietary Sandia rotary valve designed and fabricated by Rob Renzi at Sandia National Laboratories (Albuquerque, NM). Figure 6.2 describes the flow path involving the valve. The valve modulator was powered using an Agilent E3630A Triple Output DC power supply to control the modulation period. The valve was heated to 70º C using an Omega Heater Controller (CN132) with a custom housing. PEEK µTube (LabSmith, Inc., Livermore, CA) ferrules with 700 µm i.d. were used to seal the connections between the valve body and capillary tubing.

Materials and Procedures. Hydrogen carrier gas and methane for injection samples were supplied by Matheson Tri-gas. Nitrogen for the FID was sourced from house supplies. Liquid chemical samples for the 18-component separation were obtained from Fisher Scientific, Aldrich Chemical Company, Alfa Aeaser, and Acros Organics (see Table 6.1).

For the experiments, the inlet pressures ranged from 10 to 100 psig with the total flow set to 999 mL/min. The applied voltage, which controls the modulation period, to the valve ranged from 0.5 to 10.0 V. The microcolumns experienced a temperature ramp of 25º - 100º C in 10 s. Gaseous sample injections were 1 µL and liquid sample injections were 0.2 µL.

Results and Discussion

Valve Modulation Period Determination. To determine the modulation period as a function of voltage applied to the valve, a series of experiments with air injections was carried out. Voltages studied ranged from 1.0 to 10.0 V. Since the baseline level of signal produced by the FID is dependent on flow rate and the flow rate changes when the valve is opened and closed, the baseline is expected to have a sine-wave-like character. By measuring the time between signal maxima in the baseline, the period can be determined. In this study, the time between 4 to 6 periods was measured in order to get an average period value. The modulation periods ranged from 5.283 s at 1.0 V to 0.252 s at 10.0 V.

Figure 6.3 represents the relationship between the voltage applied to the valve and the resulting modulation period. On a log vs. log scale, the plot trendline is quite linear. Tests were conducted at 0.5 V but the resulting plots produced inconclusive results, so operating the valve very slowly (below 1 V) is not recommended for reproducible modulations.

Methane Modulation. A set of experiments were performed to study the influence of valve modulation rate on the 2^{nd} dimension peak width of methane for a variety of column flow rates. The modulation profiles at inlet pressures of 10, 15, 20, 25, 30, 40, and 50 psig were studied with applied voltages of 0, 2.0, 4.0, 6.0, 8.0, and 10.0 V.

It was hypothesized that the modulation profile with the greatest number of peak slices would be at the lowest flow rate with the highest applied voltage (i.e. the shortest modulation period). Figure 6.4 shows one of the modulated peak profiles that match this hypothesis – a number of peak slices arise from the methane band. The most intense peak slice has a half-height peak width of 81 ms at this flow rate.

While there were problems in getting reproducible modulation profiles due to the unknown and uncontrollable position of the valve at the start of each run, there was still a trend of fewer modulation slices as the inlet pressure increased and as the modulation period was reduced, which was the expected trend. Figure 6.5 demonstrates this since only two peak slices are produced at 40 psig inlet pressure and 4.0 V applied valve voltage. Increasing the flow rate or decreasing the modulation period beyond these conditions lead to a single methane peak exiting the modulator.

Figure 6.6 displays the half-height peak width of methane as a function of inlet pressure for various voltages applied to the valve. This data is somewhat surprising because it shows that the peak width depends much more strongly on the inlet pressure than the modulation period. It was hypothesized that the faster modulation period experiments would have the narrower peak widths, but there are examples to the contrary here. For instance, with a 25 psig inlet pressure, the narrowest peak width is sub-50 ms at 2.0 V applied to the valve, and the 4.0 V and 6.0 V settings make for progressively wider peaks. There are also instances where that hypothesis was true, such as at 40 psig inlet pressure. At that point, 2.0 V valve setting makes the widest peaks while 4.0 V and 8.0 V become progressively narrower, though not by a lot. Thus, depending on faster modulation periods for narrow peak widths is not going to work with this valve modulator design.

Peak Area Conservation. This study used a sample of n-dodecane in carbon disulfide to demonstrate that peak area is conserved when the valve modulation is applied. Figure 6.7 shows an unmodulated profile of CS2 and dodecane. The CS2 peak is split likely due to a small portion of the solvent peak going through the valve and skipping column 1 with the majority of the CS2 passing through both columns and

eluting slightly later. Figure 6.8 shows the same sample modulated with 6.0 V (437 ms period) applied to the valve.

Because the phase of the valve is uncontrolled, it must have been at least partially open when the dodecane band passed near it since there is a significant amount of dodecane eluting quite early. The portion of dodecane that did traverse both columns was modulated as expected and shows the typical modulated profile. Peak-fitting software in GRAMS was used to fit the peaks and isolate the areas of the early dodecane peak so that the total area of dodecane could be calculated.

As shown in the ANOVA analysis of Figure 6.9, there was no significant difference in the areas between the modulated and unmodulated runs at 99.99% confidence level

18 Component Separation. Figure 6.10 displays the 18-component mixture containing a variety of chemical warfare agent simulants and other molecules with a variety of functional groups. A significant portion of the two-dimensional space is occupied with peaks and the entire range of the second dimension space is being used. The true phase of the valve is not known, which likely explains the late position of a light and poorly retained molecule like CS2, but the fact remains that most of the separation space is being used. Even though the second dimension retention times are only known relative to one another, the primary retention times of the components are, as expected, correlated to boiling point.

Peak Capacity Studies. Figure 6.11 shows the 2^{nd}-dimension peak capacity calculated based on the number of theoretical plates for *n*-octane, *n*-decane, *n*-dodecane at an applied voltage of 9.0 V (277 ms modulation period) for various flow rates. This

plot shows a trend that the heavier molecules lead to slightly higher peak capacity numbers. Isothermal peak capacity is calculated using equation 6.2, where n_c = peak

$$n_c = 1 + \frac{\sqrt{N}}{4 * R} * \ln\left(\frac{t_{RL}}{t_m}\right) \tag{6.2}$$

capacity, N = number of theoretical plates, R = specified resolution (1.00 in this study), t_{RL} = retention time of the last eluting compound (size of second dimension axis), and t_m = holdup time.

Calculating N was performed using equation 6.3 where t_R = retention time of the

$$N = 5.545\left(\frac{t_R}{w_h}\right)^2 \tag{6.3}$$

compound and w_h = peak width at half-height.

Since the current generation of valves have unknown positions and thus the phase is uncontrolled, the t_m and t_{RL} of C8 were modeled through flow equations and the data files were phase shifted so C8 would elute at the modeled time.

The peak capacity equation is only applicable for isothermal conditions; therefore it cannot be used for 1st dimension peak capacity calculations. One method of peak capacity calculation is to use Trenzall (TZ) numbers instead, which provides the number of peaks that can evenly fit between two straight-chain alkane peaks. Equation 6.4

$$TZ = \left[\frac{t_{R2} - t_{R1}}{(w_h)_1 + (w_h)_2}\right] - 1 \tag{6.4}$$

describes the calculation for TZ where t_R = retention time and w_h = peak width at half-height for the earlier eluting compound (1) and the later eluting compound (2).

Figure 6.12 shows the resulting TZ numbers when using C8 as compound 1 and C12 as compound 2 for a variety of applied voltages. Again, the modulation period

change doesn't seem to cause as much of an effect on TZ as much as the inlet pressure. With higher inlet pressures and thus faster flow rates, there is less time in between the retention times of the peaks, and so less space for peaks in between and a reduced TZ.

Figure 6.13 displays a GCxGC contour plot of the 3 alkanes in CS2 with an inlet pressure of 40 psig and an applied voltage of 9.0 V (277 ms). The phase was shifted by 222 ms for this plot in order to anchor the C8 peak at the modeled expected 2nd dimension elution time. Some wrap-around is exhibited in this plot by the dodecane peak which is a result of the relatively low pressure setting. The signals displayed before 3 s result from the CS2 and is split into more than one peak due to some portion of the CS2 passing through the valve and skipping Column 1 entirely, as has been noted in the methane and peak area conservation studies.

Conclusions

A new valve modulator for high-speed comprehensive two-dimensional gas chromatography has been fabricated and tested. While the valve shows promise in its functionality, the lack of phase control is a serious problem that is being solved through a slight valve redesign. With better phase control, the valve can be in the correct configuration to block any analyte from passing through the valve and avoiding the first column, which is a current weakness of the valve. This will allow for much more reproducible chromatograms and allow for better peak capacity measurements (i.e., wrap-around situations will be much more easily proven and 2nd dimension retention correctly assessed).

Aside from that phase issue, the valve works as expected – the peak area was proven to be conserved between unmodulated and modulated situations, the relationship between applied voltage and resultant modulation period was elucidated, and even

methane was modulated with relatively good peak shapes. The 2nd-dimension peak capacity was surprisingly insensitive to flow rate, while the 1st dimension peak capacity determined through TZ showed a strong correlation with flow rate. To improve the peak capacity further, some of the dead volume within the valve will be removed in the valve redesign to prevent unnecessary band broadening. Even so, the 18-component separation already demonstrates the high-speed GCxGC separation capabilities of this system and is a promising start for a functional, high-speed GCxGC portable platform.

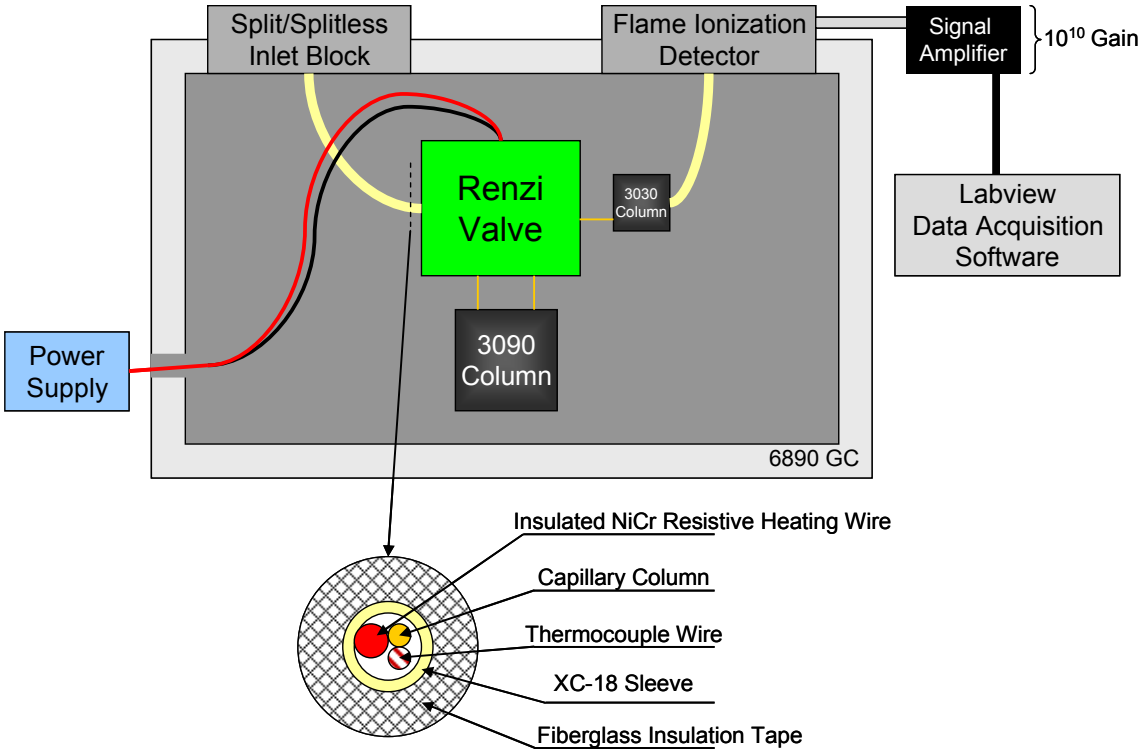

Figure 6.1 – Instrument Schematic

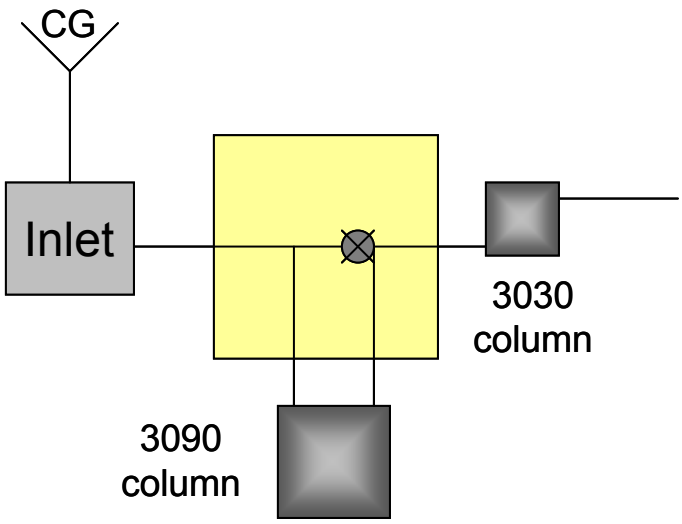

Figure 6.2 – Generic Renzi valve schematic

Table 6.1 – List of chemicals used with boiling point and commercial source

Sample #	Chemical Name	Boiling Point (° C)	Source
1	carbon disulfide	45.9	Fisher Scientific
2	toluene	111	Fisher Scientific
3	*n*-octane	126	Aldrich Chemical Co.

4	iso-octane	99	Aldrich Chemical Co.
5	1,3-dichloropropane	121	Aldrich Chemical Co.
6	dimethyl methylphosphonate	187	Alfa Aesar
7	1-octanol	195	Aldrich Chemical Co.
8	1,4-dichlorobutane	154	Aldrich Chemical Co.
9	*n*-decane	174	Aldrich Chemical Co.
10	diisopropyl methylphosphonate	219	Alfa Aesar
11	di-*n*-butyl sulfide	189	Acros Organics
12	2-chloroethyl ethyl sulfide	156	Aldrich Chemical Co.
13	1,6-dichlorohexane	204	Acros Organics
14	*n*-dodecane	216	Fisher Scientific
15	O,S-diethyl methylphosphonothioate	78*	Alfa Aesar
16	diisobutyl methylphosphonate	254	Alfa Aesar
17	2-chloroethyl phenyl sulfide	245	Aldrich Chemical Co.
18	O,S-diisobutyl methylphosphonothioate	139*	Alfa Aesar
		*= 12 mm Hg	

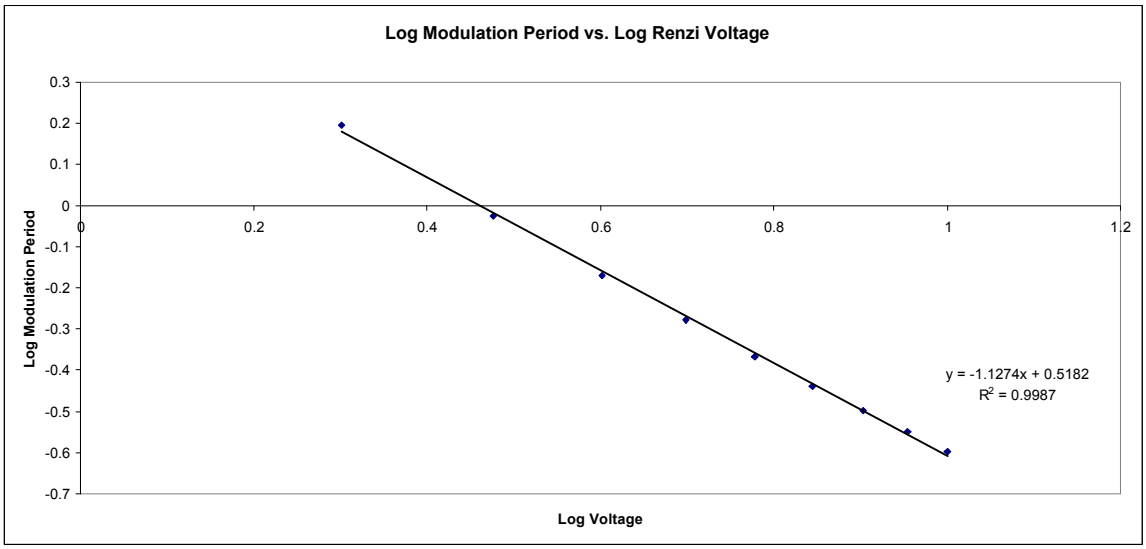

Figure 6.3 – Log of modulation period (ms) vs. log of applied voltage (V).

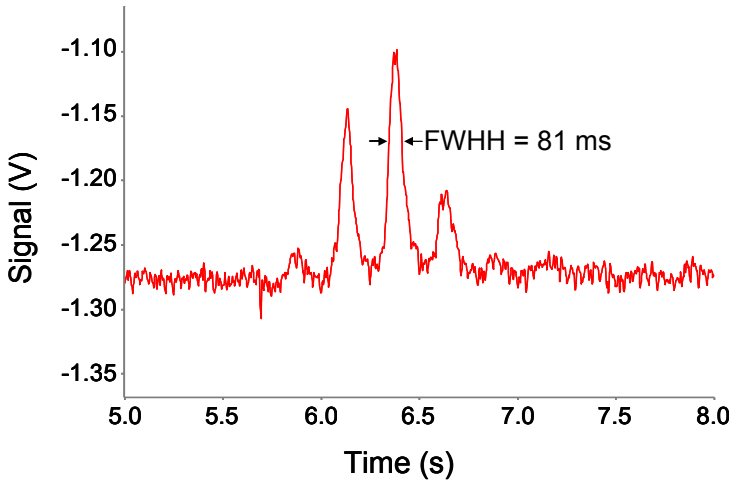

Figure 6.4 – Representative depiction of methane modulation (15 psig inlet pressure and 10.0 V applied valve voltage).

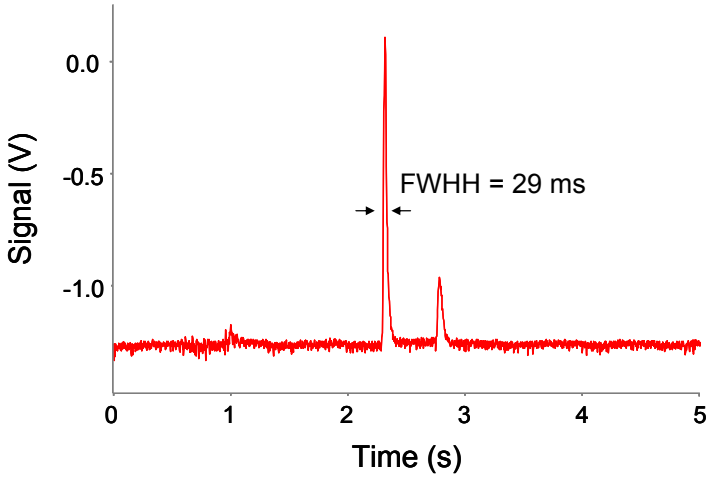

Figure 6.5 – Representative depiction of methane modulation (40 psig inlet pressure and 4.0 V applied valve voltage).

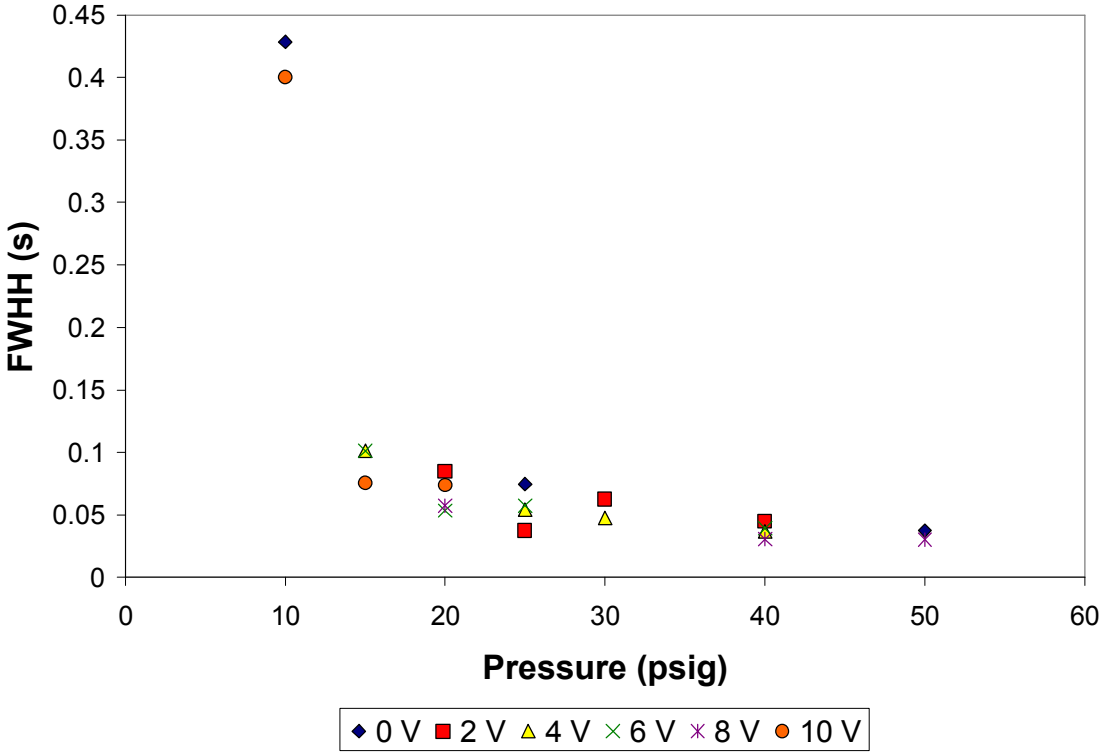

Figure 6.6 – Peak width of methane at half-height vs. inlet pressure

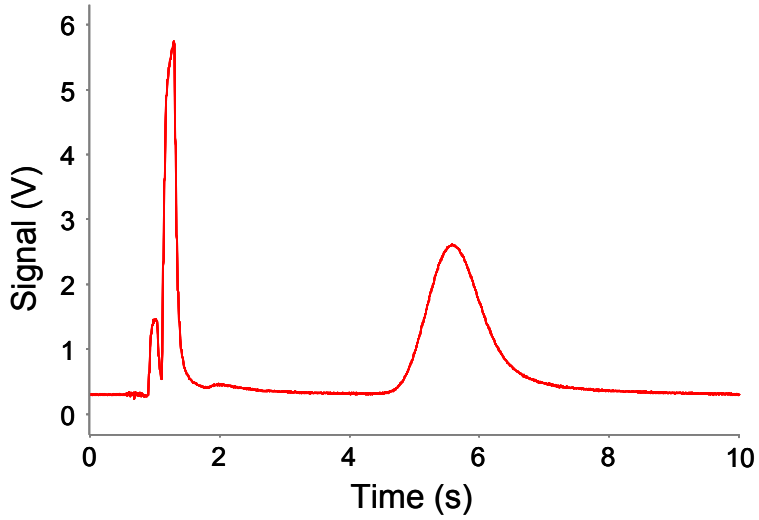

Figure 6.7- n-dodecane unmodulated

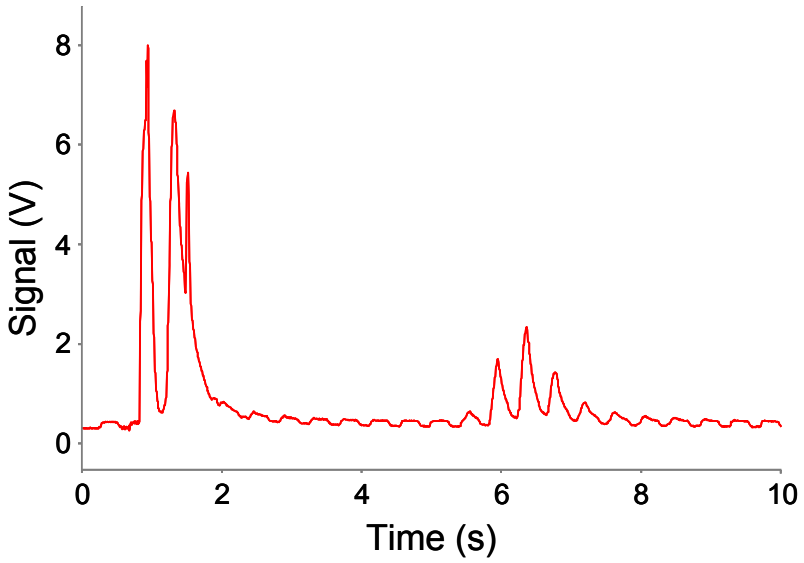

Figure 6.8 – n-dodecane modulated with 6 V applied to modulator

Run/Voltage	Off	6	8	10
1	2.3142826	2.69879892	2.1420184	2.33256065
2	2.0903842	2.4239731	2.1819499	2.10206738
3	2.4566202	2.30827295	2.340462	1.84374903

Table 6.2 Summed Peak Areas (V*s)

Figure 6.9 – Peak Area Conservation between modulated/unmodulated n-dodecane
99.99% ANOVA study from Origin

Data1_A = Valve Off
Data1_B = 6.0 V
Data1_C= 8.0 V
Data1_D= 10.0 V

One-Way ANOVA

Summary Statistics

Dataset	N	Mean	SD	SE
Data1_A	3	2.2871	0.18463	0.10659
Data1_B	3	2.47701	0.20059	0.11581
Data1_C	3	2.22148	0.10496	0.0606
Data1_D	3	2.09279	0.24454	0.14118

Null Hypothesis: The means of all selected datasets are equal
Alternative Hypothesis: The means of one or more selected datasets are different

ANOVA

Source	DoF	Sum of Squares	Mean Square	F Value	P Value
Model	3	0.230711597	0.0769038658	2.11944	0.17601
Error	8	0.290279458	0.0362849322		

At the 0.0001 level,

the population means are not significantly different

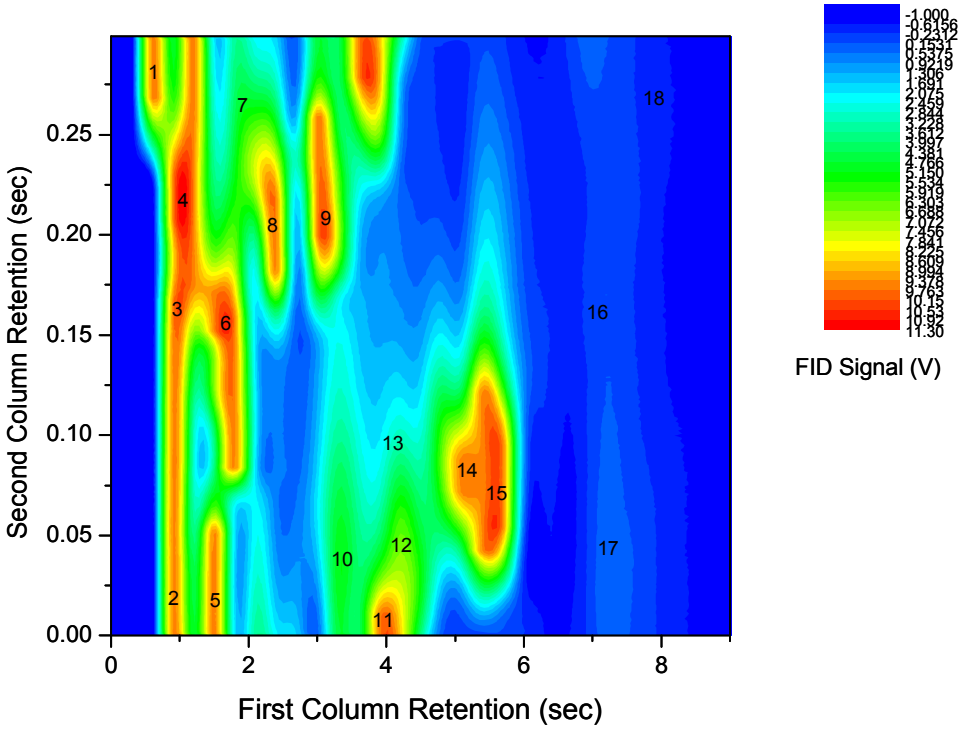

Figure 6.10 – 18 Component Separation

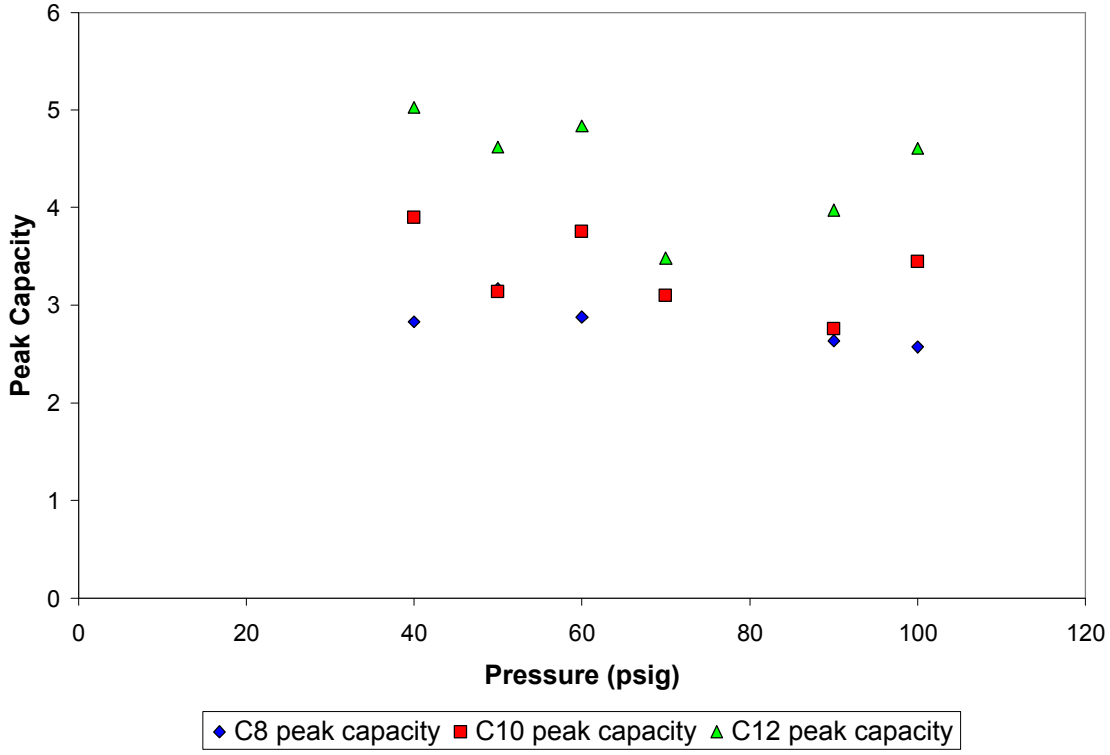

Figure 6.11 – 9.0 V Applied Voltage Maximum Peak Capacity vs inlet pressure for three n-alkanes

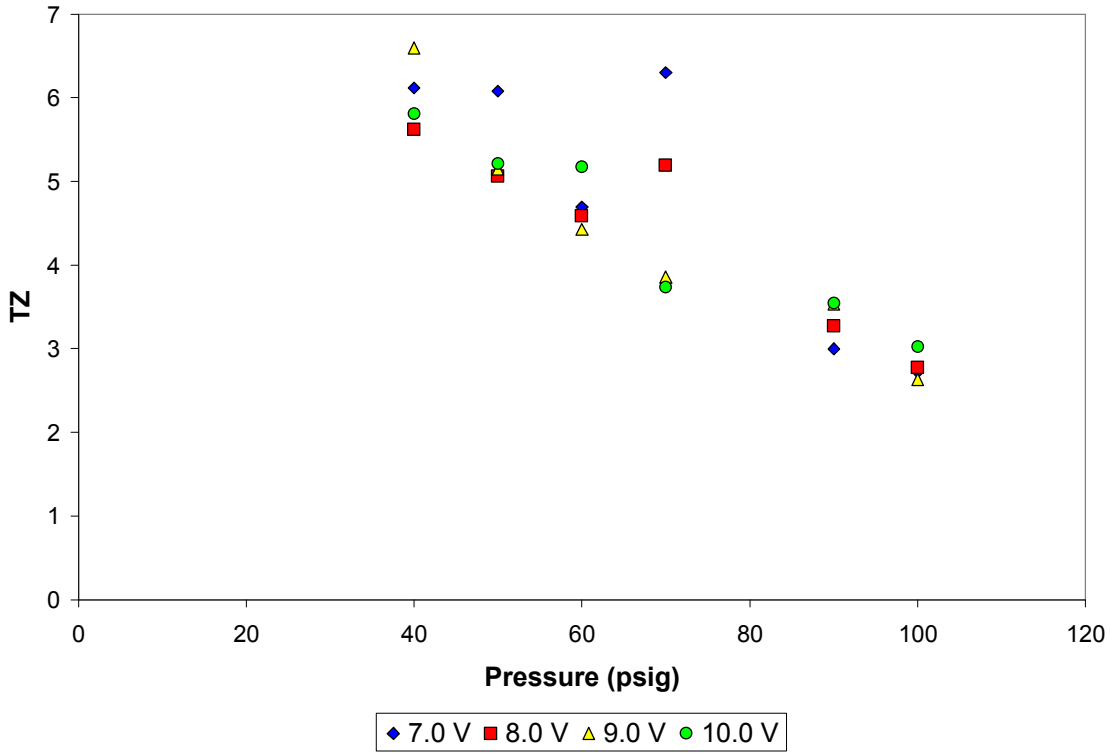

Figure 6.12 – C8-C12 TZ vs. inlet pressure for various applied valve voltages

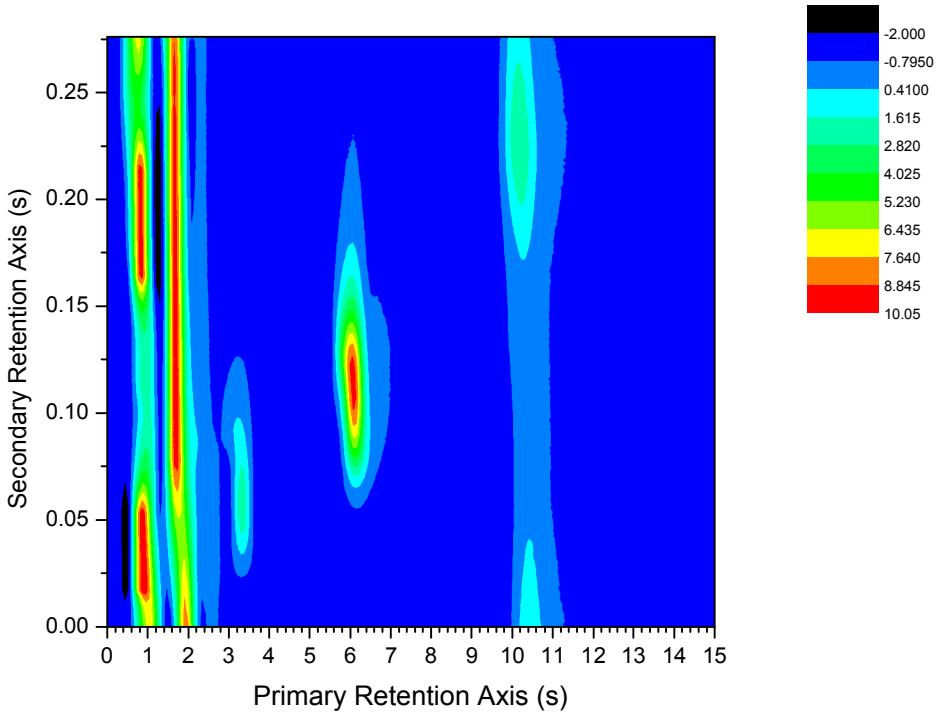

Figure 6.13 – GCxGC contour plot of C8, C10, and C12 in CS2. 222 ms phase shift employed.

References

A) Lambertus, G.; Sacks, R. *Anal. Chem*. **2005**; *77*(7); 2078-2084.

B) Whiting, J.; Sacks, R. *Anal. Chem.* **2002**; *74*(1); 246-252.

C) Veriotti, T.; McGuigan, M.; Sacks, R. *Anal. Chem*. **2001**; *73*(2); 279-285.

D) Grall, A. J.; Sacks, R. D. *Anal. Chem*. **2000**; *72*(11); 2507-2513

E) Leonard, C.; Sacks, R. *Anal. Chem*. **1999**; *71*(24); 5501-5507

F) Leonard, C.; Sacks, R. D. *Anal. Chem*. **1999**; *71*(22); 5177-5184

G) C.A. Bruckner, B.J. Prazen, R.E. Synovec, *Anal. Chem*. **1998,** *70*, 2796-2804.

H) J.V. Seeley, F. Kramp, C.J. Hicks. *Anal. Chem*. **2000**, *72*,4346-4352

I) J. V. Seeley, N. J. Micyus, S. V Bandurski, S. K. Seeley, J. D. McCurry. *Anal. Chem.* **2007**, *79*, 1840-1847.

J) T. Gorecki, J. Harynuk. *J. Sep. Sci.* **2004**, *27*, 431.